

# Breakup of $^{22}\text{C}$ studied by CDCC with Cluster-Orbital Shell-Model wave functions

*K. Ogata<sup>1</sup>, T. Myo<sup>2</sup>, T. Furumoto<sup>3</sup>, T. Matsumoto<sup>4</sup> and M. Yahiro<sup>4</sup>*

<sup>1</sup>Research Center for Nuclear Physics, Osaka University, Ibaraki 567-0047, Japan

<sup>2</sup>General Education, Faculty of Engineering, Osaka Institute of Technology, Osaka 535-8585, Japan

<sup>3</sup>RIKEN Nishina Center, Hirosawa 2-1, Wako 351-0198, Japan

<sup>4</sup>Department of Physics, Kyushu University, Fukuoka 812-8581, Japan

## Abstract

The breakup cross section (BUX) of  $^{22}\text{C}$  by  $^{12}\text{C}$  at 250 MeV/nucleon is evaluated by the continuum-discretized coupled-channels method (CDCC) incorporating the cluster-orbital shell model (COSM) wave functions. Contributions of the low-lying  $0_2^+$  and  $2_1^+$  resonances predicted by COSM to the BUX are investigated. The  $2_1^+$  resonance gives a narrow peak in the BUX, as in usual resonant reactions, whereas the  $0_2^+$  resonant cross section has a peculiar shape due to the coupling to the nonresonant continuum. Mechanism of the appearance of this shape in the breakup of  $^{22}\text{C}$  is discussed.

## 1 Introduction

Exploring the frontier of the nuclear chart is one of the most important subjects in nuclear physics. Properties of neutron drip-line nuclei, e.g.,  $^{11}\text{Li}$ ,  $^{19}\text{B}$ , and  $^{22}\text{C}$ , are therefore crucial for that purpose. Very recently, evidence for an unbound ground state of  $^{26}\text{O}$  was reported [1], which could extend the concept of drip-line nuclei to the unbound-state regions. In this situation, clarification of unbound states, i.e., resonance structures, of nuclei around the neutron drip-line will be a fascinating subject.

In this study we focus on  $^{22}\text{C}$ , the drip-line nucleus of carbon isotopes. By measuring the reaction cross section [2] and the neutron removal cross section [3], ground state properties of  $^{22}\text{C}$  have been intensively studied so far; the results strongly support the picture that  $^{22}\text{C}$  is an s-wave two-neutron halo nucleus, in consistent with the theoretical prediction of Ref. [4] based on a  $^{20}\text{C}+n+n$  three-body model. On the other hand, possible resonance states of  $^{22}\text{C}$  have never been observed and suggested.

In this paper, we investigate the resonance structure of  $^{22}\text{C}$  with the cluster-orbital shell model (COSM) [5] through the breakup cross section (BUX) of  $^{22}\text{C}$  by  $^{12}\text{C}$  at 250 MeV/nucleon evaluated by the continuum-discretized coupled-channels method (CDCC) [6–8]. COSM is a powerful method to describe a system consisting of a core plus valence nucleons; it has successfully been applied to studies of the ground and resonance states of  $^6\text{He}$ ,  $^7\text{He}$ , and  $^8\text{He}$  [9–11]. One of the most important advantages of COSM is the description of radial wave functions of each nucleon by the superposition of Gaussian basis functions, covering a quite wide space. It is thus expected that COSM describes well both resonances and the nonresonant continuum of a system, in a model space required to evaluate breakup observables. CDCC is a sophisticated reaction model that has been applied to various breakup processes with high success. Our main purpose is to investigate how the resonance states of  $^{22}\text{C}$  predicted by COSM are “observed” in the BUX.

Formalism of COSM-CDCC is described in Sec. 2 and numerical inputs are given in Sec. 2. In Sec. 3, results of the BUX of  $^{22}\text{C}$  by  $^{12}\text{C}$  at 250 MeV/nucleon are shown and discussion on the resonant and nonresonant contributions of the BUX is given. Finally, we give a summary in Sec. 5.

## 2 Formalism

In the present COSM calculation, a  $^{20}\text{C}+n+n$  three-body model is adopted for the  $^{22}\text{C}$  wave function:

$$\Phi_{cIM_I}(\boldsymbol{\eta}_1, \boldsymbol{\eta}_2) = \sum_{l_1 j_1 l_2 j_2} \sum_{i_1 i_2} d_{cl_1 j_1 l_2 j_2}^{i_1 i_2} \hat{A} \left[ \phi_{l_1 j_1}^{b_{i_1}}(\boldsymbol{\eta}_1) \otimes \phi_{l_2 j_2}^{b_{i_2}}(\boldsymbol{\eta}_2) \right]_{IM_I}, \quad (1)$$

where  $I$  and  $M_I$  are the total spin of  $^{22}\text{C}$  and its third component, respectively, and  $\boldsymbol{\eta}_i$  ( $i = 1$  or  $2$ ) is the relative coordinate of the  $i$ th neutron to the center of the  $^{20}\text{C}$  core.  $\hat{A}$  represents the antisymmetrization operator for the two valence neutrons; antisymmetrization between a valence neutron and a neutron in  $^{20}\text{C}$  is approximately taken into account with the orthogonal condition model [12].  $\phi$  in Eq. (1) is the Gaussian basis function

$$\phi_{l j m_j}^{b_i}(\boldsymbol{\eta}) = \varphi_l^{b_i}(\eta) [Y_l(\hat{\boldsymbol{\eta}}) \otimes \xi_{1/2}]_{j m_j}, \quad (2)$$

where  $\xi$  is the spin 1/2 wave function of neutron and

$$\varphi_l^{b_i}(\eta) = \sqrt{\frac{2}{\Gamma(l+3/2)}} \left(\frac{1}{b_i^2}\right)^{(l+3/2)/2} \eta^l \exp\left(-\frac{\eta^2}{2b_i^2}\right) \quad (3)$$

with  $\Gamma$  the Gamma function. The range parameters  $b_i$  ( $i = 1-i_{\max}$ ) are chosen to lie in a geometric progression:

$$b_i = b_1 \gamma^{i-1}. \quad (4)$$

By diagonalizing an internal Hamiltonian  $h$  of  $^{22}\text{C}$  with the basis functions, one obtains eigenstates, each of which is characterized by  $I$ ,  $M_I$ , and the energy index  $c$ , with the expansion coefficients  $d_{cl_1 j_1 l_2 j_2}^{i_1 i_2}$ . In the present case, there is only one bound state in  $I = 0$ . All the other states are located above the  $^{20}\text{C}+n+n$  three-body threshold, which are called pseudostates (PS).

Since COSM describes the  $^{22}\text{C}$  wave function covering a quite large model space, the PS can be regarded to a good approximation as discretized continuum states. Then the total wave function of the  $^{20}\text{C}+n+n+^{12}\text{C}$  four-body reaction system with the total angular momentum  $J$  and its third component  $M$  can be expanded as

$$\Psi_{JM}(\boldsymbol{\eta}_1, \boldsymbol{\eta}_2, \mathbf{R}) = \sum_{cIL} [\Phi_{cI}(\boldsymbol{\eta}_1, \boldsymbol{\eta}_2) \otimes \chi_{cIL}(\mathbf{R})]_{JM}, \quad (5)$$

where  $\chi_{cIL}(\mathbf{R})$  is the scattering wave of  $^{22}\text{C}$  in the  $(c, I)$  state relative to  $^{12}\text{C}$ ;  $L(\mathbf{R})$  is the corresponding relative angular momentum (coordinate).

By solving the four-body Schrödinger equation

$$[H - E] \Psi_{JM}(\boldsymbol{\eta}_1, \boldsymbol{\eta}_2, \mathbf{R}) = 0, \quad (6)$$

$$H = T_{\mathbf{R}} + U_{n_1}(\mathbf{R}_1) + U_{n_2}(\mathbf{R}_2) + U_c(\mathbf{R}_c) + h \quad (7)$$

with the standard boundary condition of  $\chi_{cIL}(\mathbf{R})$ , one may obtain the scattering matrix to the  $(c, I, L)$  channel. Here,  $E$  is the total energy of the four-body system in the center-of-mass (c.m.) frame,  $T_{\mathbf{R}}$  is the kinetic energy operator associated with  $\mathbf{R}$ ,  $U_{n_i}$  ( $i = 1$  or  $2$ ) is the neutron distorting potential, and  $U_c$  is the potential between the  $^{20}\text{C}$  core and  $^{12}\text{C}$ . This framework is *four-body CDCC* [13,14] incorporating the COSM wave functions, which we call *COSM-CDCC* below. We further adopt the prescription [15] based on the complex-scaling method (CSM) [16], the CSM smoothing method, to obtain a smooth breakup cross section  $d^2\sigma/(d\epsilon d\Omega)$ , i.e., the double differential breakup cross section (DDBUX). Here,  $\epsilon$  is the breakup energy of the  $^{20}\text{C}+n+n$  system measured from the three-body threshold and  $\Omega$  is the solid angle of the c.m. of  $^{22}\text{C}$  after the breakup; the corresponding polar angle is denoted by  $\theta$  below.

### 3 Numerical input

In the  $^{20}\text{C}+n+n$  three-body Hamiltonian  $h$ , we adopt the Minnesota nucleon-nucleon interaction [17] and a Woods-Saxon potential for the  $n$ - $^{20}\text{C}$  system, consisting of the central and spin-orbit parts. As for the latter, we use Set B parameters of Ref. [4]; we have slightly changed  $V_1$  and  $V_s$  to 20.00 MeV and 10.50 MeV, respectively, so that the  $1s$  state is unbound. In the COSM calculation, we include the single-particle configuration of each  $n$  up to  $l = 5$  ( $l = 4$ ) for the  $0^+$  ( $2^+$ ) state of  $^{22}\text{C}$ , taking into account the spin of  $n$ . The radial wave function between  $n$  and  $^{20}\text{C}$  in each single-particle orbit is described by 10 Gaussian basis functions; we use  $b_1 = 0.3$  fm and  $\gamma = 1.5$  fm in Eq. (4).

As a result of diagonalization of  $h$ , we obtain the  $0^+$  ground state at 289 keV below the  $^{20}\text{C}+n+n$  threshold, which is consistent with the experimental value  $420 \pm 940$  keV [18], together with 604 (1,385) PS above the threshold in the  $0^+$  ( $2^+$ ) state. In the CDCC calculation, we include the ground state and the 77 (164) PS for  $0^+$  ( $2^+$ ) below  $\epsilon = 10$  MeV, which are important for describing the breakup observables shown below.

As for the distorting potential of  $n$ - $^{12}\text{C}$  and  $^{20}\text{C}$ - $^{12}\text{C}$ , we adopt microscopic single and double folding models, respectively, with the CEG07b nucleon-nucleon  $G$ -matrix interaction including the medium effects [19]. We use the nuclear densities of  $^{12}\text{C}$  and  $^{20}\text{C}$  given in Refs. [20] and [21], respectively, with a slight change in the parameters for the former. CDCC equations between  $^{22}\text{C}$  and  $^{12}\text{C}$  are solved up to  $R = 30$  fm with the increment of 0.02 fm and the number of the partial waves is set to 600. In the CDCC calculation, we use the so-called no-recoil approximation to the  $^{20}\text{C}$  core, as in the previous study of Ref. [22]; this approximation is considered to be valid when the mass of the core nucleus is much larger than the valence particle(s), which is satisfied well in the present case.

In the CSM smoothing method, we adopt the complex-scaling angle of  $14^\circ$ . The basis functions used in diagonalization of the scaled Hamiltonian  $h^\theta$  are similar to those mentioned above, except that we need finer and wider bases. We show in Table 1 the number  $N$  of the Gaussian basis functions and its range parameters,  $b_1$  and  $\gamma$ , for each single-particle orbit of neutron, used in the CSM smoothing method.

**Table 1:** Parameters of Gaussian basis functions used in the CSM-smoothing method.

neutron orbit	$N$	$b_1$ (fm)	$\gamma$ (fm)
s	25	0.2	1.3
d	20	0.2	1.3
others	15	0.3	1.4

### 4 Results and discussion

Figure 1 shows the DDBUX  $d^2\sigma/(d\epsilon d\Omega)$  of  $^{22}\text{C}$  by  $^{12}\text{C}$  at 250 MeV/nucleon calculated by COSM-CDCC. One sees some structures in the DDBUX, expected to reflect properties of the resonance and the nonresonant continuum of  $^{22}\text{C}$ . In fact, COSM predicts some resonance states of  $^{22}\text{C}$  and  $^{21}\text{C}$  in the energy region shown in Fig. 1; the results are summarized in Table 2. The next question is thus how these resonances contribute to the DDBUX.

As a great advantage of the CSM-smoothing method, one can decompose the DDBUX into the components due to the three-body resonances (each of the  $0_2^+$ ,  $2_1^+$ , and  $2_2^+$  states), the binary resonance of  $^{21}\text{C}$  coupled with another neutron, and the nonresonant three-body continuum. Figure 2 shows the result of the decomposition of the breakup energy distribution  $d\sigma/d\epsilon$ , which is obtained by integrating the DDBUX over  $\theta$  from  $0^\circ$  to  $0.1^\circ$ . The left and right panels correspond to the  $0^+$  and  $2^+$  states of  $^{22}\text{C}$ , respectively. In each panel, the solid (dotted) line shows the total breakup cross section (contribution of the three-body nonresonant continuum). The contribution of the three-body resonance,  $0_2^+$  ( $2_1^+$ ) in the

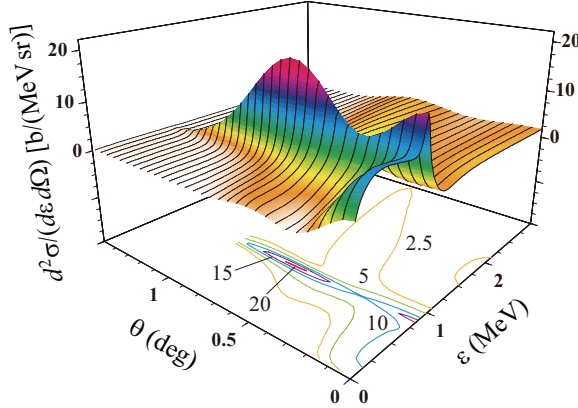


**Fig. 1:** Double differential breakup cross section (DDBUX) of  $^{22}\text{C}$  by  $^{12}\text{C}$  at 250 MeV/nucleon.

**Table 2:** Resonance energy  $E_r$  and width  $\Gamma_r$  of  $^{22}\text{C}$  and  $^{21}\text{C}$ .

nucleus	$I^\pi$	$E_r$ (MeV)	$\Gamma_r$ (MeV)	main configuration
$^{22}\text{C}$	$0_2^+$	1.02	0.52	$(0d3/2)^2$
	$2_1^+$	0.86	0.10	$(1s1/2)(0d3/2)$
	$2_2^+$	1.80	0.26	$(0d3/2)^2$
$^{21}\text{C}$	$3/2^+$	1.10	0.10	$(0d3/2)$

left (right) panel, is denoted by the dashed line. In both  $I^\pi$  states, it is found that the contributions from the  $^{21}\text{C}$  binary resonance are negligibly small. Similarly, the  $2_2^+$  resonance gives an inappreciable cross section. For the  $2^+$  state, one clearly sees that the peak in  $d\sigma/d\epsilon$  is due to the  $2_1^+$  resonance, which has the standard Breit-Wigner form. On the other hand, as shown in the left panel of Fig. 2, the  $0_2^+$  resonance has a peculiar form due to the coupling with the nonresonant continuum. It is well known that resonant cross sections can have different shapes from the standard Breit-Wigner form because of the coupling to the nonresonant continuum. This is called the background-phase effect or the Fano effect [23]. There have been many examples of the Fano effect in various research fields, e.g., neutron scattering [24], Raman scattering [25], hypernucleus formation [26], optical absorption [27], and quantum transport in a mesoscopic system [28]. Nevertheless, the sizable Fano effect on the  $0_2^+$  resonant cross section in this study should be remarked.

One of the most important characteristics of  $^{22}\text{C}$  is the dominance of the  $(1s1/2)^2$  configuration (more than 80%) in its ground state. This gives a large breakup cross section to the low-energy  $0^+$  nonresonant continuum with the same configuration, for which only the monopole transition is responsible. It should be noted that if neutron has a finite value of  $l$ , it hardly contributes to the low-energy nonresonant continuum of  $^{22}\text{C}$  because of the centrifugal barrier. At the same time, the small but non-negligible  $(0d3/2)^2$  configuration of about 13% in the ground state of  $^{22}\text{C}$  brings the low-lying  $0_2^+$  resonance. This is essentially due to the closely-located  $(1s1/2)$  and  $(0d3/2)$  single-particle orbits of  $^{22}\text{C}$ . Thus, the resonant and nonresonant states with the same spin-parity ( $0^+$ ) strongly affect each other. This is the main reason for the sizable Fano effect on the  $0_2^+$  resonant cross section. The coexistence of the  $0^+$  resonance and nonresonant continuum will rarely be realized when a core plus one neutron system is considered; an s-wave neutron cannot form a resonance, except through a compound process or a Feshbach reso-

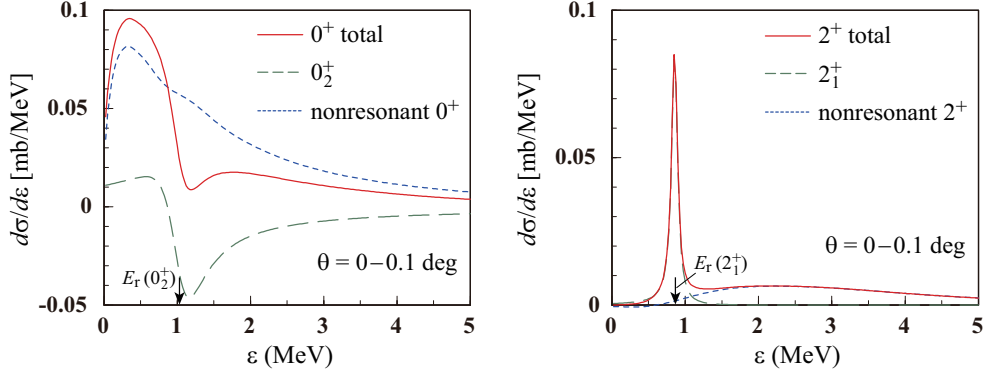


**Fig. 2:** Decomposition of the breakup energy distribution obtained by integrating the DDBUX over  $\theta$  from  $0^\circ$  to  $0.1^\circ$ . The left (right) panel is the result of the  $0^+$  ( $2^+$ ) state. The dashed lines represent the contributions of the  $0_2^+$  (left panel) and  $2_1^+$  (right panel) three-body resonances. The solid and dotted lines in each panel show the total breakup energy distribution and its nonresonant component, respectively. The arrow in the left (right) panel denotes the  $0_2^+$  ( $2_1^+$ ) resonance energy  $E_r$ .

nance [29]. Therefore, the features of the resonant cross section shown in the present study are expected to be quite unique to an  $s$ -wave two-neutron halo nucleus, i.e.,  $^{22}\text{C}$ .

Experimental data of the DDBUX of  $^{22}\text{C}$  are highly desirable to validate the interesting behavior of the  $0^+$  breakup cross section suggested here. For this purpose, one must eliminate the  $2^+$  cross section from the total DDBUX. This can be performed quite easily, because the  $2^+$  contribution will be described well by a standard Breit-Wigner form. To do this, however, we need experimental data with high energy resolution; they will hopefully be obtained at RIBF with utilizing the brand-new SAMURAI spectrometer.

## 5 Summary

We have proposed a new framework of four-body CDCC adopting COSM wave functions, *COSM-CDCC*, and applied it to the breakup process of  $^{22}\text{C}$  by  $^{12}\text{C}$  at 250 MeV/nucleon. We showed the  $2_1^+$  resonance gives a clear peak in the DDBUX, whereas the  $0_2^+$  resonant cross section has a remarkably different shape from the Breit-Wigner form. The latter is due to the coupling between the  $0_2^+$  resonance and the  $0^+$  nonresonant continuum, i.e., the Fano effect. The sizable Fano effect found in the present study is expected to be quite unique to an  $s$ -wave two-neutron halo nucleus, i.e.,  $^{22}\text{C}$ .

Experimental clarification of the sizable Fano effect on the  $0_2^+$  resonance will be very interesting. From the theoretical side, inclusion of the recoil of the core nucleus  $^{20}\text{C}$  and its dynamical excitation during the breakup of  $^{22}\text{C}$  will be important future work. Extension of COSM-CDCC to five- and six-body breakup reaction will be a very challenging subject of nuclear reaction studies.

## Acknowledgements

K. O. thanks Y. Kikuchi, K. Mizuyama, and T. Fukui for valuable discussions. T. F. is supported by the Special Postdoctoral Researcher Program of RIKEN. This research was supported in part by Grant-in-Aid of the Japan Society for the Promotion of Science (JSPS).

## References

- [1] E. Lunderberg *et al.*, Phys. Rev. Lett. **108**, 142503 (2012).
- [2] K. Tanaka *et al.*, Phys. Rev. Lett. **104**, 062701 (2009).
- [3] N. Kobayashi *et al.*, arXiv:1111.7196 (nucl-ex).
- [4] W. Horiuchi and Y. Suzuki, Phys. Rev. C **74**, 034311 (2006).
- [5] Y. Suzuki and K. Ikeda, Phys. Rev. C **37**, 410 (1988).
- [6] M. Kamimura, M. Yahiro, Y. Iseri, Y. Sakuragi, H. Kameyama, and M. Kawai, Prog. Theor. Phys. Suppl. No. 89, 1 (1986).
- [7] N. Austern, Y. Iseri, M. Kamimura, M. Kawai, G. Rawitscher, and M. Yahiro, Phys. Rep. **154**, 125 (1987).
- [8] M. Yahiro, K. Ogata, T. Matsumoto, and K. Minomo, Prog. Theor. Exp. Phys. **1**, 01A209 (2012); arXiv:1203.5392 (2012).
- [9] T. Myo, K. Kato, and K. Ikeda, Phys. Rev. C **76**, 054309 (2007).
- [10] T. Myo, R. Ando, and K. Kato, Phys. Rev. C **80**, 014315 (2009).
- [11] T. Myo, R. Ando, and K. Kato, Phys. Lett. **B691**, 150 (2010).
- [12] S. Saito, Prog. Theor. Phys. **41** (1969), 705.
- [13] T. Matsumoto, E. Hiyama, K. Ogata, Y. Iseri, M. Kamimura, S. Chiba, and M. Yahiro, Phys. Rev. C **70**, 061601(R) (2004).
- [14] M. Rodríguez-Gallardo, J. M. Arias, J. Gómez-Camacho, A. M. Moro, I. J. Thompson and J. A. Tostevin, Phys. Rev. C **80**, 051601(R) (2009).
- [15] T. Matsumoto, K. Kato, and M. Yahiro, Phys. Rev. C **82**, 051602(R) (2010).
- [16] J. Aguilar and J. M. Combes, Commun. Math. Phys. **22**, 269 (1971); E. Balslev and J. M. Combes, Commun. Math. Phys. **22**, 280 (1971).
- [17] D. R. Thompson, M. Lemere, and Y. C. Tang, Nucl. Phys. **A286**, 53 (1977).
- [18] G. Audi, A. H. Wapstra, and C. Thibault, Nucl. Phys. **A729**, 337 (2003).
- [19] T. Furumoto, Y. Sakuragi, and Y. Yamamoto, Phys. Rev. C **78**, 044610 (2008), *ibid.* **80**, 044614 (2009).
- [20] J. W. Negele, Phys. Rev. C **1**, 1260 (1970).
- [21] L. C. Chamon *et al.*, Phys. Rev. C **66**, 014610 (2002).
- [22] J. A. Tostevin and B. A. Brown, Phys. Rev. C **74**, 064604 (2006).
- [23] U. Fano, Phys. Rev. **124**, 1866 (1961).
- [24] R. K. Adair, C. K. Bockelman, and R. E. Peterson, Phys. Rev. **76**, 308 (1949).
- [25] F. Cerdeira, T. A. Fjeldly, and M. Cardona, Phys. Rev. B **8**, 4734 (1973).
- [26] O. Morimatsu and K. Yazaki, Nucl. Phys. **A483**, 493 (1988).
- [27] J. Faist, F. Capasso, C. Sirtori, K. W. West, and L. N. Pfeiffer, Nature **390**, 589 (1997).
- [28] K. Kobayashi, H. Aikawa, S. Katsumoto, and Y. Iye, Phys. Rev. Lett. **88**, 256806 (2002).
- [29] H. Feshbach, Ann. Phys. **5**, 357 (1958), *ibid.* **19**, 287 (1962).